Effect of Speckle Noise in Ultrasonic Measurement on Two-Dimensional Ultrasonic-Measurement-Integrated Blood Flow Analysis

Hiroko Kadowaki
Graduate School of Engineering, Tohoku University
6-6-01 Aramaki Aza Aoba, Aoba-ku, Sendai, Japan
kadowaki@reynolds.ifs.tohoku.ac.jp

Toshiyuki Hayase, Kenichi Funamoto, Suguru Miyauchi, Kosuke Inoue
Institute of Fluid Science, Tohoku University
2-1-1 Katahira, Aoba-ku, Sendai, Japan

Tadashi Shimazaki, Takao Jibiki, Koji Miyama
GE Healthcare Japan
4-7-127 Asahigaoka, Hino, Japan

Abstract -Information on hemodynamics is essential for elucidation of mechanisms and development of novel diagnostic methods for circulatory diseases. The authors' group developed a two-dimensional ultrasonic-measurement-integrated (2D-UMI) blood flow analysis system for easy acquisition of an intravascular blood flow field and hemodynamics using 2D-UMI simulation, which feeds back an ultrasonic measurement to the numerical blood flow simulation aiming at clinical application. Also, in a numerical experiment of three-dimensional UMI simulation, the effect of ultrasonic measurement noise assuming Gaussian distribution was examined. However, the effect of speckle noise of actual ultrasonic measurement on analysis accuracy is unknown, and the clarification of this effect is essential for clinical application of 2D-UMI simulation. The aim of this study was to clarify the effect of speckle noise in ultrasonic measurement on 2D-UMI blood flow analysis results. Ultrasonic measurement and 2D-UMI analysis for a steady flow in a circular pipe downstream of a stenosis were performed by a 2D-UMI blood flow analysis system. As a result, the optimum feedback gain was determined so that the error between the analysis result and frame-averaged measurement result of ultrasonic Doppler velocity was minimal. Finally, the 2D-UMI analysis result for the optimum gain was compared with a commonly used frame-averaged result obtained from those for higher feedback gain, and the effectiveness of the analysis result for the optimum gain was confirmed.

Keywords: Ultrasonic color Doppler measurement, Speckle noise, Measurement-integrated simulation, Blood flow analysis, *In vitro* validation.

1. Introduction

Research on arteriosclerosis has shown that it is closely related to hemodynamics (Chatzizisis et al., 2006), and information on hemodynamics is thereby essential for elucidation of mechanisms and development of novel diagnostic methods for circulatory diseases. Kato *et al*. developed a two-dimensional ultrasonic-measurement-integrated (2D-UMI) blood flow analysis system (Fig. 1(a)) for easy acquisition of information on intravascular hemodynamics aiming at clinical application, and its versatility was confirmed in various blood vessel geometries (Kato et al., 2014). Figure 1(b) shows an example of ultrasonic measurement data for the longitudinal section of blood flow in a carotid artery, the monochrome part showing a tissue image displayed in B-mode and the colored part showing the Doppler velocity of the blood flow. Figure 1(c) shows the corresponding 2D-UMI blood flow analysis result visualizing the wall shear stress and the blood flow field.

Ultrasonic-measurement-integrated simulation can correctly reproduce an intravascular blood flow field and hemodynamics by feeding back the ultrasonic measurement to a numerical blood flow simulation (Funamoto et al., 2005). In clinical ultrasonic color Doppler data used in UMI simulation, the spot-like echoes called speckle noise (also called as black holes) shown in Fig. 1(b) are generated by interference of waves which are reflected and scattered on surfaces of agglutinations of reflectors (red blood cells) sufficiently smaller than ultrasonic wavelength (about 300 μm). In a previous study (Funamoto et al., 2011), a numerical experiment of three-dimensional UMI simulation was performed to examine the effect of speckle noise assuming Gaussian noise, showing the existence of the optimum feedback gain at which the error in the analysis result is minimal according to the dispersion of the noise. However, the effect of speckle noise of actual ultrasonic measurement on analysis result is unknown, and the clarification of this effect is essential for clinical application of the 2D-UMI blood flow analysis system.

The aim of this study was to clarify the effect of speckle noise in ultrasonic measurement on the 2D-UMI blood flow analysis results. Ultrasonic measurement and 2D-UMI analysis for a steady flow in a circular pipe in downstream of a stenosis were performed using the 2D-UMI blood flow analysis system. Ultrasonic measurement data was firstly evaluated, and 2D-UMI simulations for various feedback gains were performed using this data. The optimum feedback gain was determined on the condition that the error between the analysis result and frame-averaged ultrasonic measurement data was minimal. Finally, the 2D-UMI analysis result for the optimum gain was compared with the commonly used frame-averaged result obtained from those for higher feedback gain.
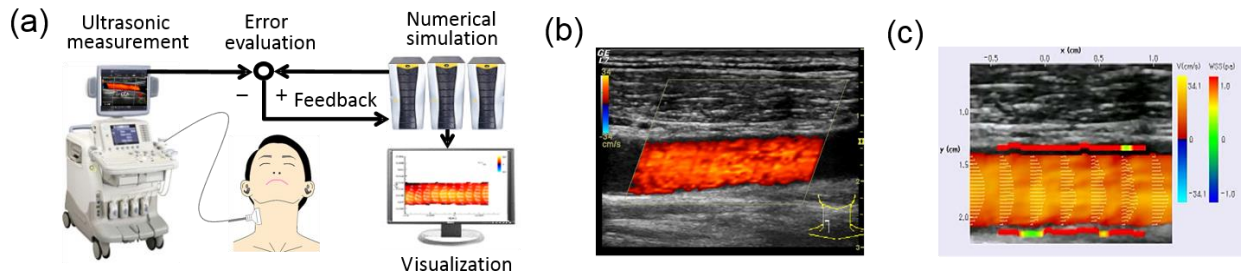

Fig. 1. (a) 2D-UMI blood flow analysis system, (b) ultrasonic measurement data, and (c) 2D-UMI blood flow analysis result.

2. Methods

2. 1. Experiment

The experimental system shown in Fig. 2(a) was composed of a constant head tank, an aluminum pipe with a stenosis at the downstream end (inner diameter $D = 8$ mm, length $L = 125D = 1000$ mm), and a polyurethane Doppler flow phantom with an inner diameter $D = 8$ mm and a length of 220 mm (ATS Laboratories, Model 524). Blood-mimicking fluid (CIRS, Model 046, density $\rho = 1.00 \times 10^3$ kg/m³,
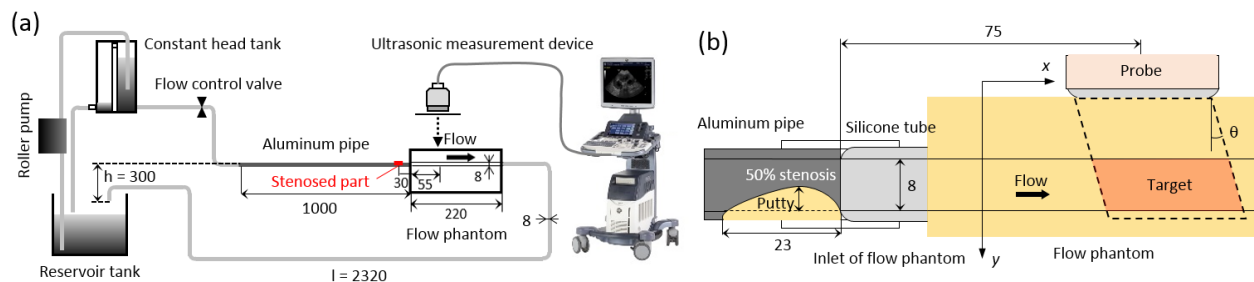

Fig. 2. (a) Configuration of experimental system and (b) detail view of a stenosis and a target flow.

kinematic viscosity $\nu = 4.0 \times 10^{-6}$ m^2/s) was circulated at a constant flow rate of 9.28 ml/s corresponding to the mean flow velocity $U = 0.185$ m/s and the Reynolds number Re $= UD/\nu = 389$, which is close to the average Reynolds number of a blood flow in a human carotid artery (Scheel et al., 2000). The connecting part between the aluminum pipe and the inflow port of the flow phantom was fixed by a silicone tube, and fifty percent stenosis of the inner diameter was created by inserting putty into the pipe for a length of 23 mm (Fig. 2(b)). Ultrasonic color Doppler measurement was performed for a steady flow of the blood-mimicking fluid in the flow phantom at a position of 75 mm (9D) in the downstream direction from the stenosis with an ultrasonic diagnostic device (GE Healthcare Japan, LOGIQ S8) with a linear type ultrasonic probe (GE Healthcare Japan, ML6-15-D). Ultrasonic measurement conditions are shown in Table 1. The dynamic range of B-mode display and the cutoff of wall filter in color Doppler mode were set to the lowest values of the device for extraction of the blood vessel shape and measurement of the low flow velocity, respectively.

Table 1. Ultrasonic measurement conditions

Frame rate [fps]	25
Acquired frame numbers	74
Measurement range [m/s]	0.17
Ultrasonic beam angle [°]	20
PRF [kHz]	2.3
B-mode frequency [MHz]	8
Color Doppler frequency [MHz]	5

2. 2. 2D-UMI Simulation

In the 2D-UMI simulation, the fluid and solid domains were binarized by superposition of time-averaged images of the B-mode and color Doppler images from the ultrasonic measurement data (Fig. 3(a)), and an orthogonal grid system for the fluid analysis was generated (Fig. 3(b)). The x-axis and y-axis in the Cartesian coordinate system were defined in the downstream direction of the vessel axis and the direction away from the body surface, respectively. The computational grid size was set according to the spatial resolution in ultrasonic measurement (see Table 2).

Governing equations of the 2D-UMI simulation are the two-dimensional unsteady incompressible Navier-Stokes equations and the pressure equation. As the external force of the Navier-Stokes equations, the artificial body force expressed as a product of the feedback gain K_V^* (nondimensional) and the difference between Doppler velocities V_m and V_c obtained by ultrasonic measurement and numerical calculation is given to each grid point in the feedback domain Ω. The feedback domain Ω was set to a position from 1/8 to 8/8 from the upstream boundary in the x-axis direction within the calculation domain (Fig. 3(b)) (Kadowaki et al., 2014). Cross-sectional average inflow velocity (inflow velocity) U of the inflow boundary condition of fluid analysis is determined so that the sum of the Doppler velocity errors in the feedback domain Ω is minimized by the golden-section search through a number of flow analyses. Inflow velocity profile was given as parabolic. The physical properties of the fluid used for the analysis were set according to the blood-mimicking fluid. The main computational conditions are shown in Table 2.

The Doppler velocities measured in the experiment and those obtained in the 2D-UMI and 2D-ordinary (2D-O) simulations were evaluated by the instantaneous-value-error $e_{Vi}(t)$ defined as the error between the computed and measured Doppler velocities at each instant in Eq. (1) and the averaged-value-error $e_{Va}(t)$ defined as the error between the computed or measured Doppler velocities at each instant and the all-frame-averaged measurement Doppler velocities in Eq. (2).

$$e_{\text{Vi}}(t) = \frac{1}{|\Omega|} \sum_{n\in\Omega} \frac{|V_c(n,t) - V_m(n,t)|}{V_{\text{type}}} \Delta\Omega \tag{1}$$

$$e_{\text{Va}}(t) = \frac{1}{|\Omega|} \sum_{n\in\Omega} \frac{|V_i(n,t) - \overline{V}_m(n)|}{V_{\text{type}}} \Delta\Omega \tag{2}$$

where V is the Doppler velocity, n is the grid index, subscripts "c" and "m" denote the computational result and the measurement data, respectively, i is c or m, V_{type} is the value of the measurement range (0.17 m/s), and $\overline{V}$ is the 74-frame-averaged value in the entire measurement time.

First, 2D-O simulation ($K_V{}^* = 0$) and 2D-UMI simulations ($K_V{}^* = 110$ and 500) were performed as typical conditions. Note that the feedback gains of 110 and 500 correspond to the minimum instantaneous- and averaged-value-errors, respectively, as shown later. Next, the optimum gain at which the error is minimal was determined by changing $K_V{}^*$ by increments of 10 from 0, and $K_V{}^*$ was changed by increments of 100 from 200 to 500.

Averaging is generally used for processing of data containing noise. The 2D-UMI analysis result for the optimum gain was compared with that obtained by averaging the results for $K_V{}^* = 500$ minimizing the instantaneous-value-error. The evaluation was performed by "M-frame averaged-value-error" $e_{\text{Va ave}}(M)$ defined as the space-averaged error between the M-frame-averaged analysis result of the Doppler velocity from the second frame except for the first frame in transition and 74-frame-averaged measurement data of the Doppler velocity.

$$e_{\text{Va ave}}(M) = \frac{1}{|\Omega|} \sum_{n\in\Omega} \frac{|\overline{V}_i(n,M) - \overline{V}_m(n)|}{V_{\text{type}}} \Delta\Omega \tag{3}$$

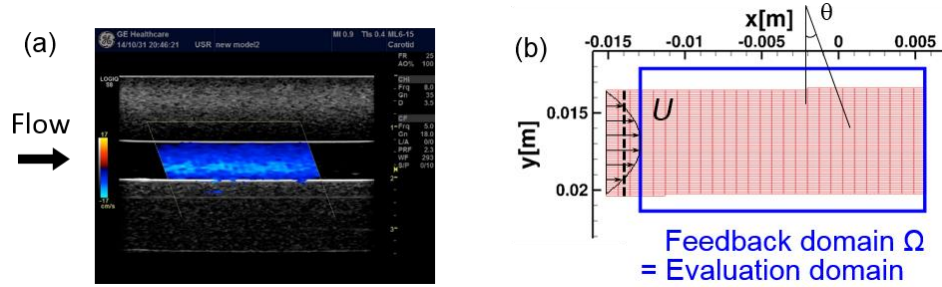where $\overline{V}_i(n, M)$ is the M-frame-averaged value of Doppler velocities from the second frame.

Fig. 3. (a) Ultrasonic color Doppler image and (b) computational grid of 2D-UMI simulation obtained from color Doppler images of a steady flow in a flow phantom.

Table 2. Computational conditions

Time step Δt [s]	0.0408
Density ρ [kg/m^3]	1.00×10^3
Kinematic viscosity ν [m^2/s]	4.00×10^{-6}
Convergence criterion of flow analysis	1.00×10^{-4}
Convergence criterion of gold section search	1.00×10^{-3}
Grid numbers $N_x \times N_y$	28×128
Grid spacings $\Delta x \times \Delta y$ [μm]	775×145

3. Results and Discussion

3. 1. Ultrasonic Measurement

An example of Doppler velocity distribution of the blood-mimicking fluid measured by the color Doppler mode in the experiment is shown in Fig. 4(a). The one-frame measurement image of the figure is nonuniform as a whole due to speckle noise. Figure 4(b) is the flame average of all 74 measurement data. The state of the flow deflected to the lower side due to the upstream stenosis appears clearly. Figure 4(c) is the spatial distribution of the standard deviation of the Doppler velocity measurement. A larger variation occurs in the lower side where the flow velocity is high. The space-averaged value of the standard deviation is 0.028, which is normalized by the value used in the numerical experiment of a previous study (Funamoto et al., 2011) (0.32 m/s) and is close to 0.022 assumed in the previous study. In this study, the 74-frame-averaged Doppler velocity distribution was regarded as that of a true flow field and was used as the standard for evaluation of the analysis and measurement results.
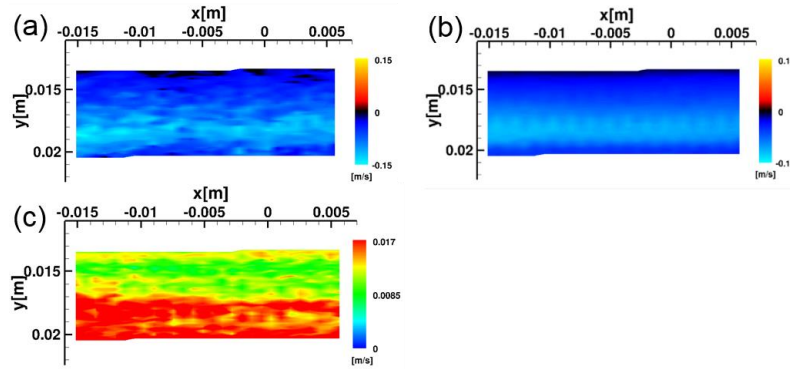

Fig. 4. Doppler velocity measurement shown in distributions of (a) one frame result ($t = 0.408$ s), (b) 74-frame-averaged result, and (c) standard deviation.

3. 2. 2D-UMI Simulation

Time variations of the instantaneous-value-errors e_{Vi} of 2D-O simulation ($K_V^* = 0$) and 2D-UMI simulations ($K_V^* = 110$ and 500) are shown in Fig. 5(a). The value of the 2D-O simulation is larger than those of 2D-UMI simulations, and the time variation is large. The error of the 2D-UMI simulation decreases with increasing feedback gain from 110 to 500.

Time variations of the averaged-value-errors e_{Va} for the above-mentioned cases and measurement data are shown in Fig. 5(b). In 2D-O simulation, results in three time steps in the beginning correspond to the convergence transition in the unsteady numerical simulation, and the results are almost steady after
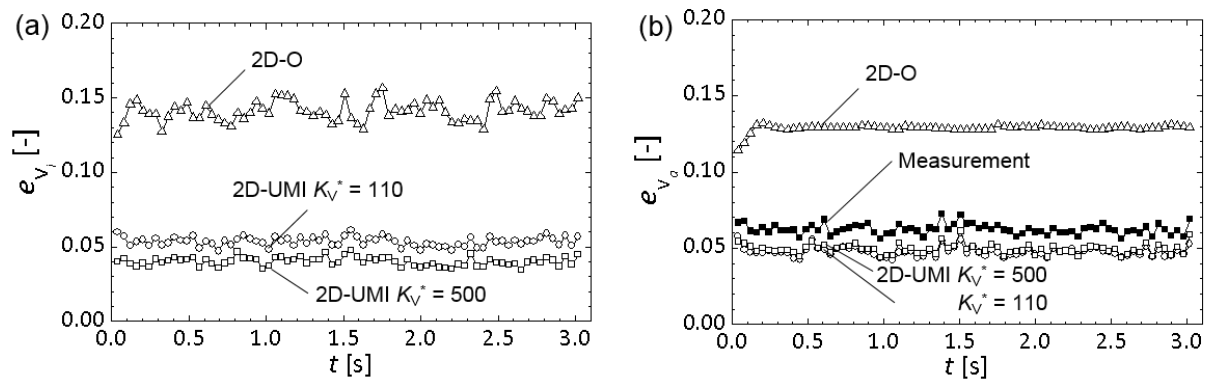

Fig. 5. Time variations of (a) instantaneous-value-errors and (b) averaged-value-errors.

these frames. The error of 2D-O simulation is slightly smaller than its instantaneous-value-error, and the time variation is relatively small. The error of 2D-UMI simulation for $K_V^* = 110$ is slightly smaller than that for $K_V^* = 500$. In comparison with the instantaneous-value-errors, the error for $K_V^* = 110$ is smaller but that for $K_V^* = 500$ is larger than corresponding averaged-value-errors, respectively. The error of measurement data is 20% larger than those of 2D-UMI simulations. This is because the noise component of measurement data is larger than those of 2D-UMI simulations.

The velocity vectors and Doppler velocity distributions of the analysis results at $t = 0.408$ s (same instant as Fig. 4(a)) are shown in Figs. 6(a)-(c). The result in Fig. 6(d) is described later. The velocity profile of the 2D-O simulation in Fig. 6(a) maintains a parabolic profile given at the upstream boundary toward the downstream end. As for that of 2D-UMI simulation for $K_V^* = 110$ in Fig. 6(b), the velocity profile of the flow field deflected to the lower side due to the upstream stenosis is properly reproduced in the feedback domain. Although the deflected velocity profile is also reproduced in the 2D-UMI simulation for $K_V^* = 500$ in Fig. 6(c), the velocity profile is rough, probably became the speckle noise of the measurement data is reproduced in the result. Consequently, it is considered that the result of 2D-UMI simulation for $K_V^* = 110$ is more proper than that for $K_V^* = 500$.
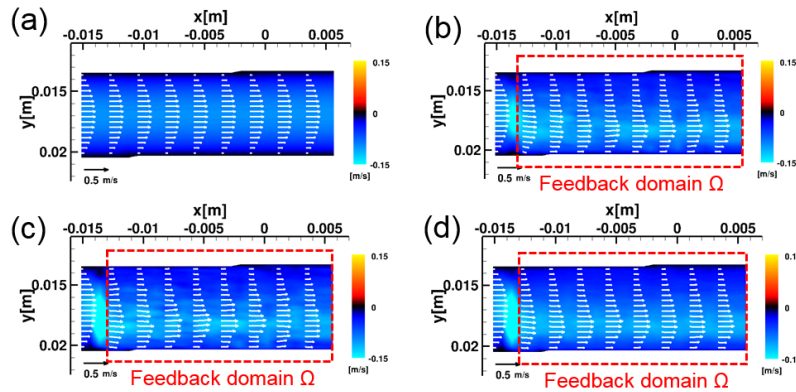

Fig. 6. Velocity vectors and Doppler velocity distributions for the analysis results. Instantaneous velocity fields at $t = 0.408$ s of (a) 2D-O simulation ($K_V^* = 0$), 2D-UMI simulations for (b) $K_V^* = 110$ and (c) $K_V^* = 500$. (d) 9-frame-averaged velocity field of 2D-UMI simulations for $K_V^* = 500$.

The feedback gain at which the error due to speckle noise was minimal was determined. Variations of the time average of the instantaneous-value-errors and those of averaged-value-errors with the feedback gain are shown in Fig. 7. The error bar shown in each plot gives the standard deviation of the error. The instantaneous-value-error $\bar{e}_{Vi}$ in Fig. 7(a) monotonically decreases with increasing feedback gain and
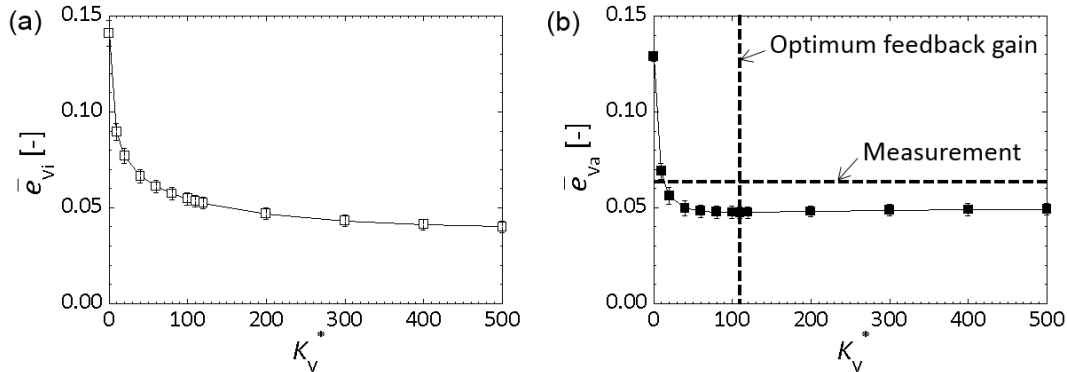

Fig. 7. Variations of (a) the time-average of the instantaneous-value-errors and (b) those of the averaged-value-errors with feedback gain.

becomes minimal at $K_V{}^* = 500$ in the present condition. On the other hand, the averaged-value-error $\bar{e}_{Va}$ in Fig. 7(b) decreases with increasing feedback gain, becomes minimal at $K_V{}^* = 110$ and gradually increases to $K_V{}^* = 500$. These results show the same trend as those of the numerical experiment of the previous study (Funamoto et al., 2011). The optimum feedback gain was determined for actual ultrasonic measurement data as $K_V{}^* = 110$ so that the averaged-value-error of Doppler velocity is minimal.

3. 3. Frame Averaging

Variations of the error of M-frame averaged-value-error (M-frame error) for Doppler velocity with average frame number M are shown in Fig. 8 for the measurement data, 2D-O simulation, and 2D-UMI simulations for $K_V{}^* = 100$ and 500. The error at $M = 1$ is evaluated using one frame data without averaging and is the same as the above-mentioned averaged-value-error $e_{Va}(t)$ evaluated at the second frame. The one-frame error decreases in the order of 2D-O simulation, measurement data, 2D-UMI simulation for $K_V{}^* = 500$, and that for $K_V{}^* = 110$, whereas the 9-frame error decreases in the order of 2D-O simulation, 2D-UMI simulation for $K_V{}^* = 100$, that for $K_V{}^* = 500$, and measurement data. The 9-frame errors are smaller than 1-frame errors except for the 2D-O simulation. Moreover, the 9-frame error of 2D-UMI simulation for $K_V{}^* = 500$ is close to that of the measurement data. According to the above results, it is shown that the error decreases with increasing feedback gain and the optimum gain does not exist for 9-frame averaging results in the present condition. The 9-frame average for the velocity field of 2D-UMI simulation for $K_V{}^* = 500$ is shown in Fig. 6(d). There is little difference between the result for the optimum gain $K_V{}^* = 110$ in Fig. 6(b) and the 9-frame-averaged result in Fig. 6(d). These results show that the frame averaging efficiently reduces the effect of speckle noise but that it generally degrades the time resolution. Considering the application of unsteady blood flow analysis, 2D-UMI result using one frame data with the optimum gain is considered to be effective.
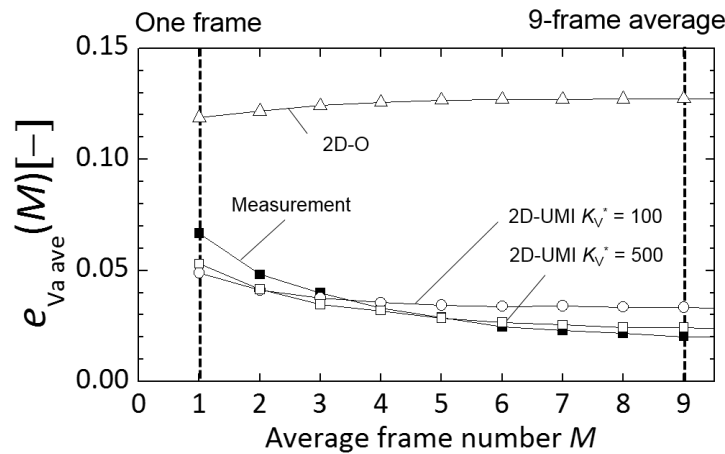

Fig. 8. Variations of the M-frame averaged-value-errors with average frame number M for measurement, 2D-O, and 2D-UMI simulations.

4. Conclusions

In order to clarify the effect of speckle noise in ultrasonic measurement on 2D-UMI blood flow analysis results, ultrasonic measurement and 2D-UMI analysis for a steady flow in a circular pipe in downstream of a stenosis were performed by a 2D-UMI blood analysis system. As a result, the optimum feedback gain was determined so that the error of ultrasonic Doppler velocity between the 2D-UMI analysis result and the frame-averaged measurement result was minimal. Finally, the 2D-UMI analysis result for the optimum feedback gain was compared with commonly used frame-averaged result obtained from those for higher feedback gain, and the effectiveness of the analysis result for the optimum gain was confirmed.

Acknowledgements

References

Chatzizisis, Y.S., & Giannoglou, G.D. (2006). Pulsatile Flow: A Critical Modulator Of The Natural History Of Atherosclerosis. *Medical Hypotheses,* 67(2), 338-340.

Funamoto, K., Hayase, T., Shirai, A., Saijo, Y., & Yambe, T. (2005). Fundamental Study Of Ultrasonic-Measurement-Integrated Simulation Of Real Blood Flow In The Aorta. *Annals of Biomedical Engineering,* 33(4), 415-428.

Funamoto, K., Hayase, T., Saijo, Y., & Yambe, T. (2011). Numerical Analysis Of Effects Of Measurement Errors On Ultrasonic-Measurement-Integrated Simulation. *IEEE Transactions on Bomedical Engineering,* 58(3), 653-663.

Kadowaki, H., Hayase, T., Funamoto, K., & Taniguchi, N. (2015). Study Of Estimation Method For Unsteady Inflow Velocity In Two-Dimensional Ultrasonic-Measurement-Integrated Blood Flow Simulation. *IEEE Transactions on Bomedical Engineering,* submitted.

Kato, T., Funamoto, K., Hayase, T., Sone, S., Kadowaki, H., Shimazaki, T., Jibiki, T., Miyama, K., & Liu, L. (2014). Development And Feasibility Study Of A Two-Dimensional Ultrasonic-Measurement-Integrated Blood Flow Analysis System For Hemodynamics In Carotid Arteries. *Medical & Biological Engineering & Computing,* 52(11), 933-943.

Scheel, P., Ruge, C., & Schöning, M. (2000). Flow Velocity And Flow Volume Measurements In The Extracranial Carotid And Vertebral Arteries In Healthy Adults: Reference Data And The Effects Of Age. *Ultrasound in Medicine & Biology,* 26(8), 1261-1266.